WC-Co High Energy Thermal Sprayed Coatings†

— Structures and Mechanical Properties —

Yoshiaki ARATA*, Akira OHMORI** and Eishi GOFUKU

Abstract

Coatings of WC-Co system alloys have been applied by thermal spraying to add wear resistance to metal substrates. However, compared with sintered WC-Co alloys, conventional plasma sprayed coatings carried out in air do not possess satisfactory mechanical properties, possibly due to the fact that tungsten carbides decompose in a high temperature plasma jet.

Three types of spraying methods (conventional plasma spraying in air, high energy gas flame spraying and low pressure plasma spraying) are examined, and the relation between the structure and mechanical property of the coatings produced by each spraying method is discussed.

In the high energy spraying process, the decomposition of WC in WC-Co powders involves a thermal activation reaction which results in dissociation of the carbon. This reaction is accelerated in an oxygenating atmosphere.

The Vickers hardness of WC-Co sprayed coating can be described by the product of two factors—the dispersion hardening strengthened by WC particles and layer binding strength affected by melted W produced by the WC decomposition reaction.

KEY WORDS: (High Energy Thermal Spraying) (Coating) (Structure) (Mechanical Properties) (WC-Co Alloy)

1. Introduction

Usually, WC-Co system alloys are produced by the powder metallurgical method. Since these alloys possess high wear resistance, they are very suitable as the tool materials. Recently, the thermal spraying method has drawn particular attention as a surface coating technique, and coatings of WC-Co system alloys have been applied by thermal spraying to add wear resistance to metal substrates. However, compared with sintered WC-Co alloys, conventional plasma sprayed coatings carried out in air do not possess satisfactory mechanical properties, possibly due to the fact that tungsten carbides decompose in a high temperature plasma jet.[1)]

In this paper, three types of spraying methods (conventional plasma spraying in air, high energy gas flame spraying and low pressure plasma spraying) are examined and the structures and mechanical properties of the coatings produced by each spraying method are discussed.

2. Experimental Procedures and Materials

2.1 Thermal spraying equipment and procedures

A PLASMADYNE (Mach 1, 40 kW-class) was used for conventional plasma spraying, with argon and helium serving as the plasma operation gases. Typical spraying conditions are shown in **Table 1**.

The gun of the high energy gas flame spraying equipment is shown schematically in **Fig. 1**. First, the pilot lamp gas, hydrogen is introduced into the mixture chamber and ignited. Oxygen and the fuel gas (70% acetylene + 30% propylene) are introduced into the chamber, then a high temperature and high pressure are generated by the continuous detonation. Spraying powder is then introduced into the nozzle by nitrogen carrier gas, heated and accelerated. Compared with a plasma jet, the gas flame temperature is lower (about 3,000°C), but the velocity of the sprayed particles is estimated at above Mach 2. Typical spraying conditions are shown in **Table 2**.

† Received on Nov. 9, 1985

* Professor
** Associate Professor
*** Graduate Student (Materials and Electronic Devices LAB. Mitsubishi Electric Corp.)

Transactions of JWRI is published by Welding Research Institute of Osaka University, Ibaraki, Osaka 567, Japan

Table 1 Conventional plasma spraying conditions.

Spraying apparatus	Plasmadyne (Mach 1)
Arc gas (Ar)	3.5 kg/cm^2
Auxiliary gas (He)	7.0 kg/cm^2
Powder feed gas (Ar)	3.5 kg/cm^2
Hopper setting	1.5 RPM
Volts	34 - 35 V
Amps	600,800,900 A
Spraying distance	100 mm
Scan speed of gun	87 mm/sec

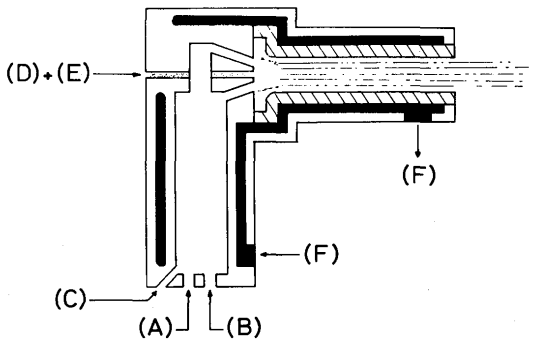

Fig. 1 Gun for the high energy gas flame spraying.

Table 2 High energy gas flame spraying conditions.

Spraying apparatus	JET-KOTE
Fuel gas (WELCUT)	2.5,3.0,3.5,4.0 kg/cm^2
Oxygen gas	5.5 kg/cm^2
Powder feed gas (N_2)	2.0 - 3.0 kg/cm^2
Nozzle size	152 mm x 79 mm
Spraying distance	150 mm
Scan speed of gun	87 mm/sec

Low pressure plasma spraying equipment is shown schematically in **Fig. 2**. The plasma spraying gun was a METCO (7 MB, 70 kW-class), and argon and hydrogen served as the plasma operation gases. Spraying was carried out in a low pressure argon atmosphere. The spraying conditions are shown in **Table 3**.

2.2 Materials

Alumina sand blasted SUS304 steel was used for the spraying substrate. Three types of commercial WC-Co system powders were sprayed: WC-12%Co (A-type), WC-12%Co (B-type) and WC-17%Co (C-type).

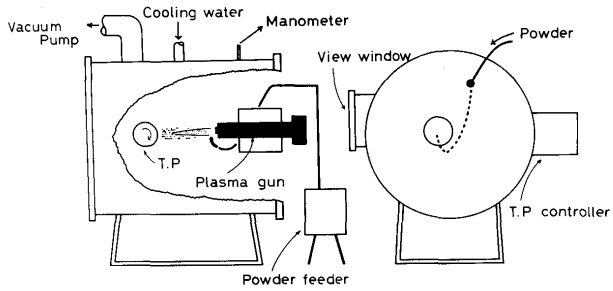

Fig. 2 Low pressure plasma spraying equipment.

Table 3 Low pressure plasma spraying conditions.

Spraying apparatus	METCO (7MB)
Spraying atmosphere	Ar,100 Torr.
Arc gas (Ar)	7.0 kg/cm^2,200 SCFH
Auxiliary gas (H_2)	4.9 kg/cm^2,15 SCFH
Volts	70 V
Amps	500 A
Spraying distance	200 mm

2.3 Analysis of the coatings

The structures of the powder before spraying and of the sprayed coating after spraying were examined by SEM and EDX, and the phases were determined by X-ray (Cu, $K_{\alpha 1}$) diffraction.

3. Results and discussions

3.1 Structure of the WC-Co system powders before spraying

Results of SEM and EDX examination of the WC-Co system powders before spraying are shown in **Fig. 3**. The grain sizes of the A-type and B-type powders are approximately same, and the grain size of the C-type powder is 2–3 times that of the A-type and B-type.

According to the EDX results, there are two separate regions in each particle. Only W can be detected in one region, but both W and Co can be detected in the other region. X-ray diffraction showed that region (1) of the A-type is WC, and region (2) is Co_3W_3C; region (1) of the B-type is WC or $W_6C_{2.54}$, and region (2) is Co_3W_3C, or Co solid soluted W; and region (1) of the C-type is WC, while region (2) is WC solid soluted Co. These results are summarized in **Table 4**. **Figure 4** shows a phase diagram of a vertical section of the carbon corner of the metastable W-Co-C system.[2] The W-Co ratio is 57/43. With regard to the carbon content, the composition of the A-type powder is that of region (14) in the phase diagram, the composition of the B-type powder corresponds to that of region (18–20), and the composition of the C-type powder is the same as that of region (6). The carbon con-

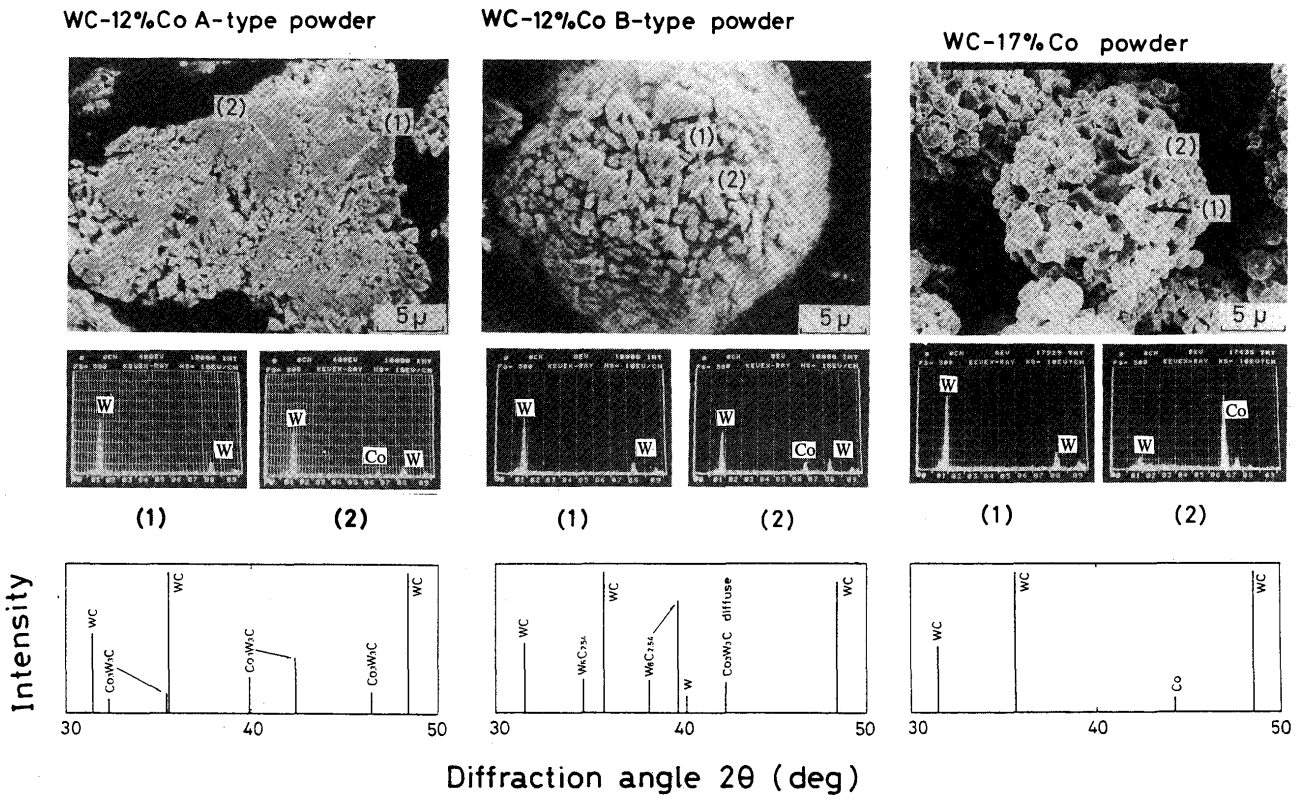

Fig. 3 Microstructures, EDX analysis results and X-ray diffraction patterns of three types of WC-Co system powders. A-type (left) B-type (center) C-type (right)

Table 4 Phase of four types of WC-Co system powders.

Type	Composition	Phases
A-type	WC-12%Co	WC, Co_3W_3C ;14
B-type	WC-12%Co	WC, $W_6C_{2.54}$, W, Co_3W_3C, $Co_xW_yC_z$;18-21
C-type	WC-17%Co	WC, β-Co ;6
D-type	A-type +Carbon	WC, Co_3W_3C, C

tent of these powders successively increases in the following manner: B-type A-type C-type. Furthermore, an additional D-type was defined as graphite powder added to the A-type.

3.2 Structures of conventional plasma sprayed coatings

During the plasma spraying process, the small particles in the spray are exposed to a high temperature atmosphere. (The temperature of the plasma jet is about 15,000°C). Thermal decomposition of the spraying material and the reaction with the high temperature gas greatly affect the characteristics of the coating. In the case of conventional plasma spraying process in air, the sprayed particles (WC-Co) are remarkably active in the plasma jet. Since the sprayed particles can easily react with the large amount of oxygen in the air contaminating the plasma jet, the decomposition of carbides cannot be avoided.

Typical X-ray diffraction results for B-type and C-type conventional plasma sprayed coatings are shown in **Fig. 5**.

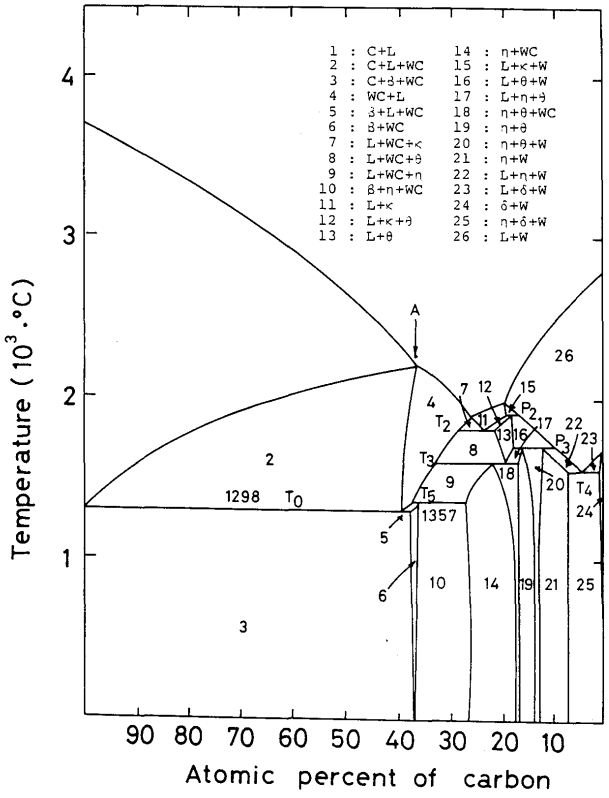

Fig. 4 Phase diagram of W-Co-C system alloy.

The results for the powders before spraying are shown underneath. The decomposition of the carbides in the B-

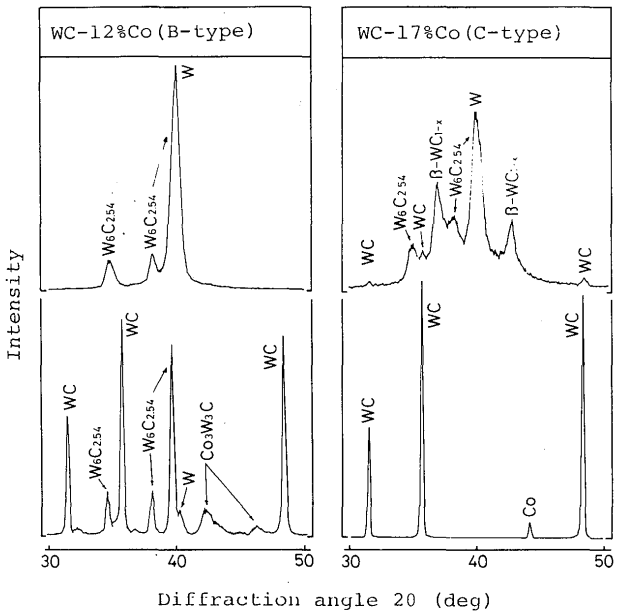

Fig. 5 X-ray diffraction results for B-type and C-type conventional plasma sprayed coatings.

type sprayed coating is remarkable, and the phases constituting the coatings are W and $W_6C_{2.54}$. Before spraying, the C-type powder processes the largest amount of carbon in the form of carbides, nevertheless, WC decomposes to β-WC_{1-x}, except for W and $W_6C_{2.54}$. From these results, the reaction of the WC-Co particles can be described as "moving to the right-hand side of the phase diagram". (see Fig. 5).

Generally, WC-Co system alloys are dispersion hardening materials. Therefore any decrease in WC dispersion particle will result in deterioration of the mechanical properties of the coating. In the conventional plasma sprayed coatings WC particles are almost nonexistant. For suppression of WC decomposition and improvement of the mechanical properties, the following methods were considered.

(1) Suppression of WC decomposition by reducing the temperature of the spraying heat sources.
(2) Suppression of WC decomposition by increasing the spraying particles' velocity.
(3) Suppression of WC reaction with oxygen by providing a nonoxygenating environment.
(4) Increasing the carbon content of the sprayed powders.

It may be considered that the method (1) and (2), can be achieved by high energy gas flame spraying, and method (3) is achieved by low pressure plasma spraying.

3.3 Structure of high energy gas flame sprayed coatings

Fig. 6 shows the X-ray diffraction results of high energy gas flame sprayed A-type and B-type coatings under the conditions shown in Table 2, changing the fuel gas pressure P_F. The results for powders before spraying are shown underneath. It can be seen that for both A-type and B-type coating, the diffraction intensity of WC decreases and that of W increases as P_F is raised. Under the same spraying conditions and P_F, A-type powder, which contains a larger amount of carbon than the B-type before spraying, possesses a large amount of carbides than the B-type in the coating.

In high energy gas flame spraying process, it may be considered that a rise in P_F increases the gas flame

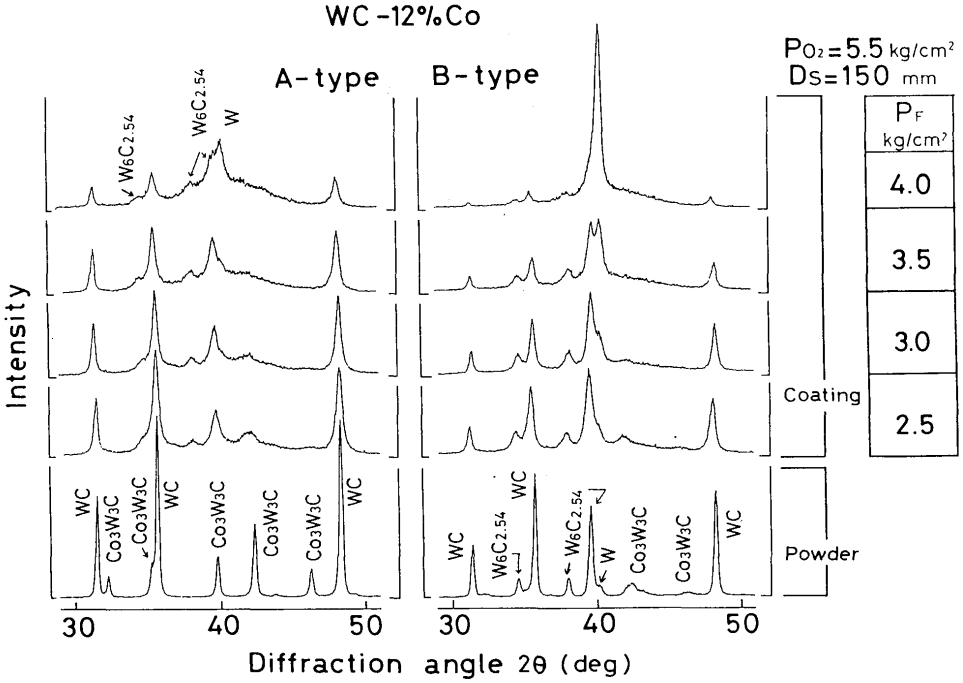

Fig. 6 X-ray diffraction results for A-type and B-type high energy gas flame sprayed coatings, changing the fuel gas pressure P_F.

temperature rather than the gas flame velocity. The amount of WC decomposition increases as P_F is raised in an oxygenating environment.

The effect of P_F on the diffraction pattern of the high energy gas flame sprayed C-type coating, which possesses the largest amount of carbon in the form of carbides before spraying, is shown in **Fig. 7**. In contrast with the A-type and B-type coatings, there is no significant decrease in WC intensity as P_F is raised. Furthermore, the reaction of β-Co with WC results in WC-Co compounds.

Figure 8 shows the X-ray diffraction results for D-type (graphite powder added to A-type) and A-type high energy gas flame sprayed coatings under the same spraying conditions. Compared with the A-type coating, WC decomposition in the D-type coating is suppressed by the addition of graphite powder. However, it was not impossible that even the addition of so large an amount of graphite powder, that carbon is retained in the coatings, cannot completely suppress the WC decomposition.

In this way, when compared with conventional plasma spraying, it was found that the high energy gas flame spraying process is able to suppress WC decomposition, and that carbon has an observable effect on WC decomposition. However, it is very easy for WC to react with the spraying atmosphere; i.e., with the oxygen in air.

3.4 Structure of low pressure plasma sprayed coatings

In high temperature heat sources, WC-Co particles are fused. If it was not for dissociation into carbon and tungsten through the reaction with oxygen, the liquid would return to the same metastable state as before spraying. WC-Co system hard alloys are usually produced by sintering WC and Co particles in a hydrogen or vacuum atmosphere. Since the liquid produced at the grain boundaries returns to a metastable state without carbon dissociation during slow cooling, binding of the grain boundaries is guaranteed. If the same phenomena were to occur in the thermal spraying process, the dispersed tungsten carbides particles would bind more strongly with the coating matrix rectify the most serious defects of the thermal sprayed coatings, namely, the weekness of the interface between stacked layers.

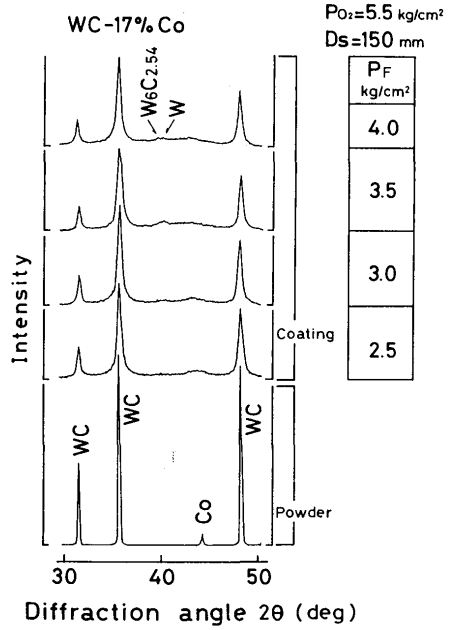

Fig. 7 X-ray diffraction results for C-type high energy gas flame sprayed coatings, changing the fuel gas pressure P_F.

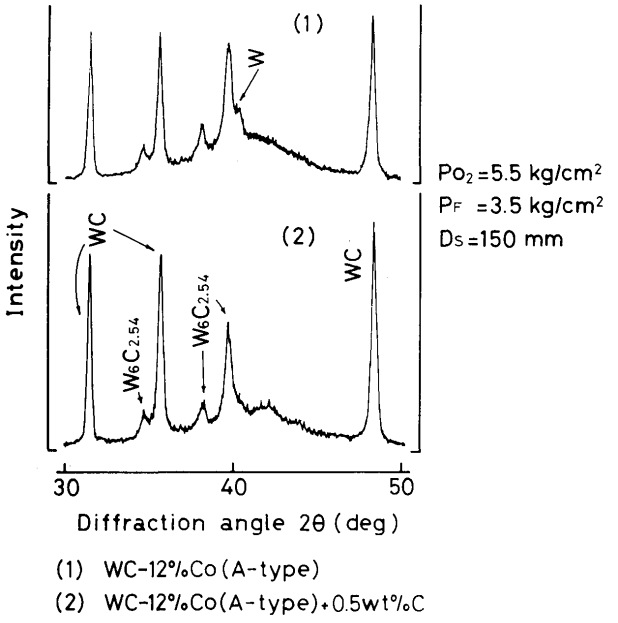

Fig. 8 X-ray diffraction results for A-type and high energy gas flame sprayed coatings.

Figure 9 shows the X-ray diffraction results for A-type and B-type low pressure plasma sprayed coatings which differ from the sprayed coatings produced in air. There is no decomposition of the tungsten carbides in low pressure plasma sprayed coatings. Furthermore, Co_3W_3C is transformed into Co_6W_6C. Since they have the same crystalline structure (tetragonal, Fd3m), Co_3W_3C can be transformed into Co_6W_6C by the production of vacancies without the lattice transformation. So, the low pressure plasma spraying processes is able to produce sprayed coatings without serious decomposition of the carbides.

3.5 Mechanical properties of the coatings

Figure 10 shows the effect of the fuel gas pressure P_F on the Vickers hardness of A-type and B-type high energy gas flame sprayed coatings. They were tested under a load of 300 g for 30 seconds. The mean values and standard deviations of 20 samplings are shown in this figure. The Vickers hardness of the coatings increased as the tungsten carbides content decreased (see Fig. 6). Usually, if there was no change in the size of dispersion particles in dispersion hardening alloys, the hardness decreased as the number of the dispersion particles decreased. Interestingly, the hardness of the sprayed coatings therefore

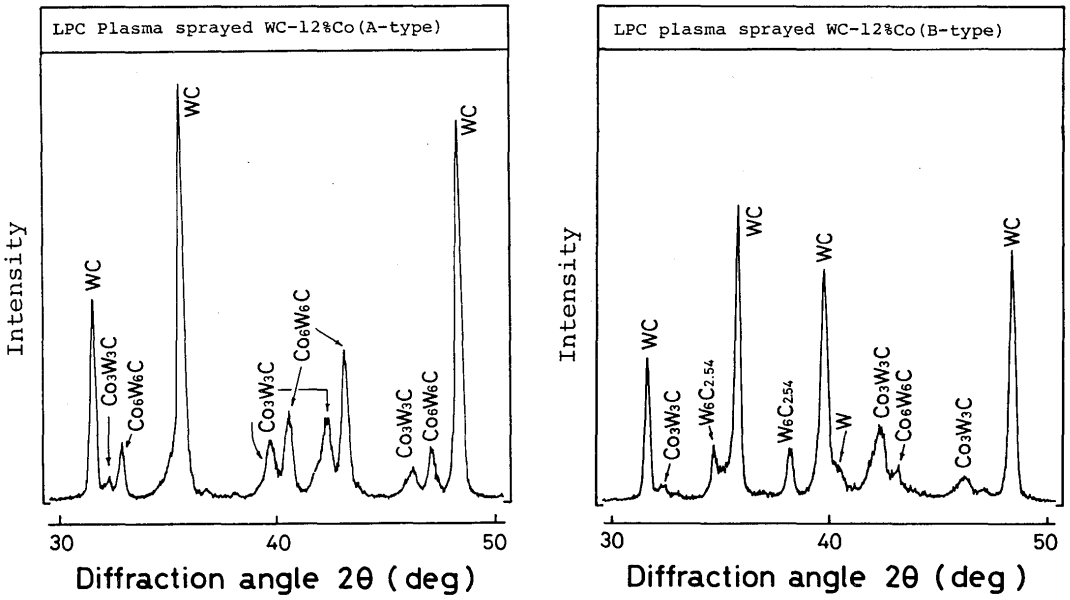

Fig. 9 X-ray diffraction results for A-type and B-type low pressure plasma sprayed coatings (D_S = 200 mm, W_P = 35 kW, P_{ch} = 100 Torr).

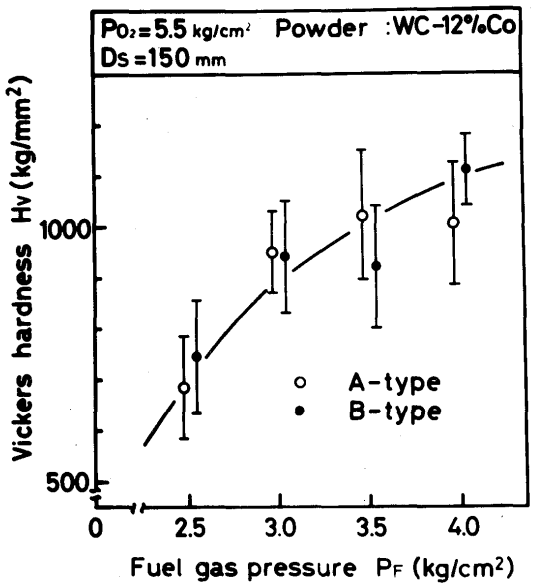

Fig. 10 Effect of P_F on the Vickers hardness of A-type and B-type high energy gas flame sprayed coatings.

shows a tendency opposite to that of conventional dispersion strengthened materials. Compared with sintered materials, this specificity of mechanical properties appears to be due to the way, the layer binding strength of the sprayed coating is estimated.

By fractography of the sprayed coatings, it was clarified that fractures of sprayed coatings propagate through the interface of the stacked layers, and that the interfaces are strengthened by the reaction products produced in the spraying process, such as melted W. In other words, the hardness of WC-Co system sprayed coatings can be described as the product of two factors the dispersion hardening and the layer binding strength. There is no relation between the dispersion hardening and the heat input into the sprayed particles (in this paper, corresponding to P_F and W_P), but there is a positive relation between the layer binding strength and the heat input. Therefore, the hardness of high energy gas flame sprayed coatings depends on the layer binding strength, rather than on dispersion hardening.

Figure 11 shows the effect of the fuel gas pressure P_F on the Vickers hardness of C-type high energy gas flame sprayed coatings. There is no significant change in the amount of WC when P_F changes (see Fig. 7). Nevertheless, the hardness of C-type sprayed coatings increases as P_F is raised, because the interfaces of stacked layers are strengthened by WC and β-Co compounds. The addition of graphite powder somewhat suppressed WC decomposi-

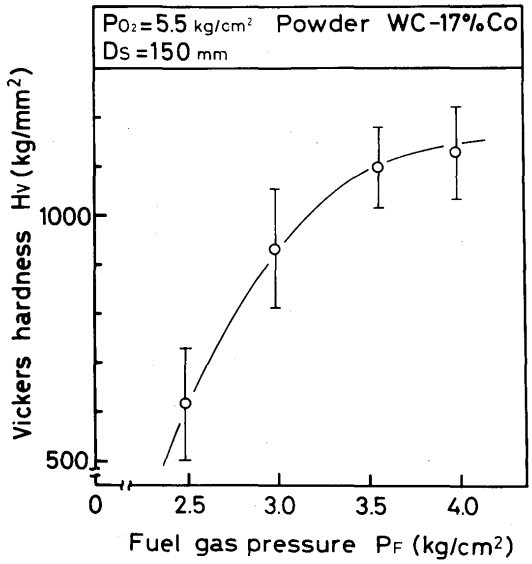

Fig. 11 Effect of P_F on the Vickers hardness of C-type high energy gas flame sprayed coatings.

tion in the D-type coating. However, no change in the hardness was observed, because of the weak layer binding strength.

Figure 12 shows the effect of the electrical output W_P on the Vickers hardness of B-type and C-type conventional plasma sprayed coatings. In contrast to high energy gas flame sprayed coatings, the hardness of conventional plasma sprayed coatings decreases as W_P increases, and the hardness of conventional plasma sprayed coatings depends on the dispersion hardening, rather than on the layer binding strength. In the case of high heat input to sprayed particles in an oxygenating atmosphere such as in the conventional plasma spraying process, the melted W resulting from WC decomposition strengthens the stacked layer interfaces. However, as there is a large decrease in dispersion particles, the hardness is greatly affected by the resoltant decrease in the dispersion hardening.

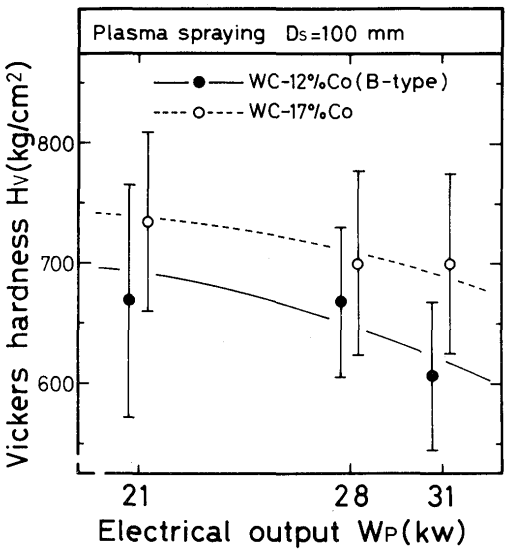

Fig. 12 Effect of W_P on the Vickers hardness of B-type and C-type conventional plasma sprayed coatings.

The average Vickers hardness of B-type low pressure plasma sprayed coatings was 1,230 ± 70 Hv. The maximum and the minimum were, 1,776 Hv and 608 Hv, respectively. It may be considered that the scatter results from a large number of porosities. However the porosities can be decreased by the improvement of the spraying conditions. The maximum (1776 Hv) corresponds to that of sintered materials. This hardness is obtained because there is no decrease in dispersion hardening at the same time that the stacked layer interfaces are strengthened by the high heat input to the sprayed particles.

Figure 13 shows an idealized model for the hardness of WC-Co system sprayed coatings. The vertical axis and the abscissa are the Vickers hardness and heat input to the sprayed particles, respectively. The hardness can be described by the product of the two factors previously discussed. Therefore, the hardness of WC-Co system

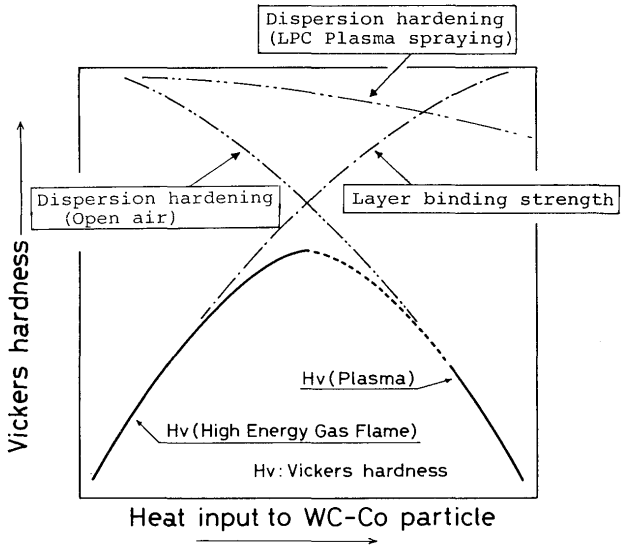

Fig. 13 Idealized model for the hardness of WC-Co system alloy sprayed coatings produced by three types of spraying.

sprayed coatings is characterized by a convex parabolic relation to the heat input. The changes accompanying variations in P_F and W_P, can thus be uniformly explained by this model. Furthermore, in order to improve mechanical properties of WC-Co sprayed coatings, it is obvious that both of these factors must be considered at the same time.

4. Conclusion

In high energy spraying process, the decomposition of WC-Co involves a thermal activation reaction, which results in dissociation of the carbon. This reaction is accelerated in an oxygenating atmosphere.

The Vickers hardness of WC-Co sprayed coatings can be described by the product of two factors the dispersion hardening and the layer binding strength.

In this paper, the authors have tried to construct an easy to understand model of the mechanical properties of WC-Co sprayed coatings. Future studies will require closer investigation of the microstructure of coatings and establishment of new testing methods.

Acknowledgement

The authors would like to thank Mr. R. Nagayama for his valuable cooperation in conducting the experimental work.

References

1) V.I. Kostkov and U.A. Shesterin, Plasma Spraying; Nisso Tsushinsha, 1981.

2) P. Rautala and J.T. Norton, Tungsten-Cobalt-Carbon System; J. of Met. 1045, 1952.